UNIUNEA EUROPEANĂ

GUVERNUL ROMÂNIEI
MINISTERUL MUNCII, FAMILIEI ȘI PROTECȚIEI SOCIALE
AMPOSDRU

Fondul Social European
POS DRU 2007-2013

Instrumente Structurale
2007-2013

MINISTERUL EDUCAȚIEI CERCETĂRII TINERETULUI ȘI SPORTULUI
OIPOSDRU

UNIVERSITATEA ALEXANDRU IOAN CUZA IAȘI

„Al. I. Cuza" University
Faculty of Physics

CONTRIBUTION IN THE MAGNETOMETRY DOMAIN

SCIENTIFIC LEADER,

Prof. univ. dr. Octavian Ioan BALTAG

PhD student,

Anca BĂNĂRESCU (married IFTEMIE)

Iassy, March 2014

The thesis presents the results of the research financially supported from European social funds managed by the Management Authority for the Sectorial Operational Program Development of Human Resources 2007- 2013 [RO08- POSDRU 6/1.5/S/25] "Development of the opportunities offered to postgraduates for flexible trajectories in carrier"

CONTENT

The summary of the PhD Thesis preserves the numbering of chapters and figures, tables and bibliographic indications.The summary of the PhD Thesis preserves the numbering of chapters and figures, tables and bibliographic indications from the thesis

Introduction

During the recent years the interest concerning the study of magnetic fields produced by bioelectric activity has increased. This research field is named biomagnetism and it has brought its contribution to the development of the devices for biomagnetic field detection.

The only laboratory in Romania where biomagnetic researches can be performed is the Laboratory of Bioelectromagnetism that belongs to the "Gr. T. Popa" University of Medicine and Pharmacy of Iassy, the Faculty of Medical Bioengineering.

Chapter 1
State of art in biomagnetometry researches

1.1. Field definition

The biomagnetism studies the generation of the magnetic fields produced by living organisms. Biomagnetometry is dealing with the non-invasive detection and measurement of the magnetic fields produced by these, as well as with the determination of tissues magnetic susceptibility. One can thus detect and measure the magnetic field generated through electrophysiologic processes.

Biomagnetism implies the measurement and analysis of the magnetic fields produced by living organisms, fields whose order of magnitude is much smaller than the ambiental magnetic field. In this work the applications of biomagnetometry and magnetometric techniques in clinical medicine and diagnosis will be presented.

1.2. Ambiental electromagnetic field. Notions of electromagnetic compatibility

During the last hundred years, the humanity participated in the biggest technological progress until now. All these new devices and installations meant to increase the degree of comfort are the main source of artificial electromagnetic disturbances that did not existed a hundred years ago.

1.3. Methods for diminishing the ambiental magnetic field

The natural and artificial ambiental magnetic fields are about 8 orders of magnitude higher than the biomagnetic fields. Therefore, in order to measure a biomagnetic field of the order of 10^{-12} T, it is necessary to reduce the ambiental field down to around the same value. The spectrum of the ambiental electromagnetic field is very complex due to various sources of disturbances that disturb the natural electromagnetic environment, such that shielding or compensation solutions were looked for each frequency spectrum.

1.3.1. Ferromagnetic shielding

The first shielded enclosure of big dimensions was realized by Patton and Fitch in 1962 [22]. In 1967 at the University of Illinois, Chicago, Cohen realized a shielded room consisting of two ferromagnetic layers and an aluminum layer having a shielding factor of 400 in the range of very low frequencies (VLF), and in 1970 at the Massachusetts Institute of Technology of Historical Interest, a shielded room was developed, consisting of five layers, of which three 1.6 mm thick layers were of high permeability magnetic material (permalloy) and two 6.3 mm thick layers were made of pure aluminum. This room had a shielding factor of 2000 for low frequencies and a good shielding of the urban noise, but the execution price was very high [15].

1.3.2. Shielding through eddy currents

Eddy currents are local induction currents that appear in metallic parts when they are subjected to variable magnetic fluxes. The eddy currents concentrate close to the surface of the conducting material, their intensity exponentially decreasing with the distance from the magnetic field source.

1.3.3. Shielded rooms

The shielded rooms destined to biomagnetometry study are enclosures with relatively big dimensions (of the order of meters) which provide attenuation of the external disturbing electromagnetic fields and of other static or time variable disturbing fields.

1.3.4. Methods for active shielding of magnetic fields

Active shielding (active, dynamic compensation) is performed by a system that works in a negative feed-back loop. These systems are used to obtain minimum values of the magnetic fields in a well-defined volume.

1.4. Devices destined for detection and measurement of biomagnetic fields

The very small values of the biomagnetic fields are detectable by means of SQUID (Super Quantum Interference Device) type magnetometers. The SQUID magnetometers mostly used in biomedical domain are those of HTS (High Temperature) type that works at the temperature of liquid nitrogen of 77 K or LTS (Low Temperature) that works at the temperature of liquid helium of 4.2 K.

1.4.1. Phenomenon of superconductibility

The superconductibility phenomenon consists in the annulment of the electric resistance of some compounds when they are cooled down to a certain transition temperature, T_c (the resistance is not really annulled, but it reaches such small values, that is considered negligible).

1.4.2. Meissner Effect

The Meissner effect was discovered in 1933 by the German physicists W. Meissner and R. Ochsenfeld, and consists in rejection of the magnetic flux by a superconducting body at the moment when this is introduced in the magnetic field.

1.4.3. Josephson Effect

The Josephson Effect consists in tunneling pairs of electrons from a superconductor layer to another through an insulating layer placed between the two. The ensemble of the two superconductors separated by a dielectric represents a Josephson junction through which, under certain conditions, a superconducting current can flow, whose value is influenced by the presence of a magnetic field. This is the effect on which the operation of the SQUID device is based.

1.4.4. Field quantization

The magnetic field quantization consists in the fact that the magnetic flux passing through a surface bounded by a contour (a superconducting ring) takes discrete values, integral multiples of the parameter Φ_o, named magnetic flux quantum ($\Phi, = n\ \Phi_o$).

1.4.5. SQUID magnetometer destined to biomagnetometry studies

The SQUID (Superconductor Quantum Interference Device) magnetometer is the device with the best sensitivity used to measure the biomagnetic fields. As the biomagnetic fields have values of (10-11 – 10-15) T, their detection and recording need the utilization of superconducting materials.

1.4.6. Flux- voltage transformer

A SQUID type magnetometer works as a magnetic flux- to- voltage transducer transforming a magnetic flux, more difficult to measure, in an electric voltage, an easy to measure parameter.

1.4.7. SQUID Gradientmeter

In order to detect the biomagnetic fields in a partially shielded medium, it is recommendable to use gradientmeters that consist in a detection coil coupled with an input coil which, in turn, is inductively coupled with the SQUID sensor.

1.5. Medical applications of biomagnetometrry

1.5.1. MCG magnetocardiography

The magnetocardiography (MCG) represents the graphical recording of the variations of the magnetic field determined by the heart electric activity. Magnetocardiography is a non-invasive method to detect and measure at the body surface the magnetic field generated by the heart electric activity. Generally, the magnetic field generated by the spontaneous heart activity at the thorax surface has values of (1 ÷ 100) pT within the frequency range (0.1 ÷ 100) Hz.

1.5.2. Magnetoencephalography (MEG)

As a non-invasive method, MEG permits the localization of epileptic focuses and to perform neurological studies concerning visually and acoustically evoked fields, as well as the evoked pain generated fields [70].

1.5.3. Biosusceptometry

The standard methods used for the evaluation of leaver overloading with iron, as well as in the case of genetic diseases such as haemochromatosis and beta thalasemia, are invasive (hepatic biopsy). In exchange, this method permits a non-invasive detection of the iron deposits from the human organism.

1.5.4. Magnetic markers

The magnetic markers and tracers are used to study the gastro-intestinal motilities.

1.5.5. Magnetopneumogram MPG

The methods used to detect the Fe_3O_4 particles consists in the application, in the direction of thorax, of a magnetic field that will magnetize the particles accumulated in the lungs, and then in the measurement of the residual magnetic field of these previously magnetized particles [101, 102].

1.5.6. Magnetogastrogram and magnetoenterogram

By means of the SQUID magnetometers one can record the magnetic fields produced by the spontaneous electric activity of the digestive tract, or by the contraction of stomach or intestine muscles.

1.5.7. Studies on peripheral nerves

The propagation of the potential of action of the electrically stimulated nervous fibers generates a magnetic field that can be detected by placing a magnetometer with one channel or a plane network of magnetic sensors [73, 74].

1.5.8. Cytomagnetometry

Cytomagnetometry is a relatively recent technique that permits to measure the dynamics of the magnetic moments of the Fe_3O_4 particles, in order to investigate the mechanisms of intracellular motions and cytoplasm mechanical properties [75].

1.5.9. Studies of foetal biomagnetometry

One of the most useful applications of the biomagnetism is the non-invasive measurement of the heart and brain fetal activity.

1.5.10. Fetal magnetocardiography fMCG

The magnetic field of the fetus heart can be detected even it is only of the order of (0.5÷10) pT, as compared to the magnetic field of the mother's heart, which is about 50 pT.

1.5.11. Cross-vaginal fetal magnetocardiography

Tristan Technologies, USA, has developed recently a trans-vaginal probe by whose means one can detect the magnetic component of the fetal cardiac activity starting with the 13^{th} week.

1.5.12. Fetal magnetoencephalography (fMEG)

The detection of fMEG can only be performed by highly sensitive bio-magnetometers with a big number of channels.

1.6. Techniques for biomagnetic signals processing and interpretation

Here are some representative examples of techniques used for biomagnetic signal processing:

- analysis of the main components [125- 128];
- Wavelet transform [129,130];

- Spatial separation of signals [131]
- Classification of the multiple signals [132, 133];
- Spatial filtration [134].

1.7. Modeling the biomagnetic sources

Modeling represents a fundamental human activity: in order to reflect the world, the human brain needs to create models; the human thinking is a modeling thinking, meant to extend the understanding of nature by "refining" (and generalizing) some distinctive parts of the Universe, irrespective of their magnitude and of our previous experience over them.

1.8. National and international tendencies

The worldwide tendency is to create measuring systems with more and more channels that should cover a wider and wider area of interest, meant to produce the magnetic mapping of various organs or anatomic regions. A mobile system was already created in the United States of America located in a laboratory built on the platform of a truck, with a view to carry out biomagnetometry studies at any place [67]. At the same time, investigations are performed on materials for shielding the enclosures where biomagnetometry installations are operating, with a view to obtain the highest damping factors possible.

Chapter 2
Theoretical and experimental researches concerning the genesis of cardiac magnetic field

2.1. Preliminary notions

The living cell possesses certain electric properties because great part of the component molecules from the intra- and extra-cellular mediums are in a dissociated state, under the form of ions with unequal intra- and extra-cellular distributions.

2.2. Heart

The heart is one of the most important organs of the human body and it works like a muscular pump that distributes the blood to the entire organism.

2.2.1. Heart configuration

The heart consists of four cavities, namely two atriums and two ventricles. In a simplified representation, the heart can be compared with a truncated cone with its top directed downward, forward to the left, its size being almost the size of individual fist.

2.3. Electric phenomena at heart level

2.3.1. Electric activity of cardiac muscular cells

In the excitable cells, the electric signals are carried first of all by trans-membrane ionic currents that modify the trans-membrane potential. The ions motion through the trans-membrane channels is governed by the laws of physics.

2.3.2. Nernst potential. Relation between the diffusion potential and ionic concentration difference

Because the ions concentrations on the two sides of the cellular membrane are not equal to each other, they tend to diffuse according to the concentration gradient toward the medium with the lower concentration. As the ions are electrically charged, their displacement is influenced by the trans-membrane electric field. The trans-membrane potential difference at which the thermodynamic diffusion force is equal to the electric force is known as equilibrium potential.

2.3.3. Mathematical modeling of cardiac electrophysiology- Cell membrane- RC circuit

The trans-membrane channels can be considered as variable resistances in series with a condenser which represents the cellular membrane. From an electrodynamics point of view, the cellular membrane and the ionic trans-membrane channels, together with the electrochemical gradients associated to each type of ions can be assimilated to a RC circuit.

2.4. Excito-conducting systems

The excito-conducting system consists of myocardium cells with specific properties, such as the automatism (they spontaneously generate an electric impulse) and conducting the impulse.

2.4.1. Heart electrophysiology

The electric activity of the heart during a cardiac cycle comprises the generation of a stimulus within the sino-atrial nodule and its transmission in the entire myocardium.

2.4.2. Genesis of electrocardiogram

The electrocardiogram represents the graphical recording of the electric potential vibrations generated at the heart surface due to the cardiac activity. Each myocardium contraction is the result of the electric excitation originating from the sinusal nodule and transmitted to the heart muscles.

2.4.3. Electrocardiographic derivations

The electrodes that pick up the potentials generated by the heart activity are located in various points on the body surface. A certain ratio between the points of electrodes locations defines a derivation.

2.5. Properties of human tissue

The general characteristics of the medium are:

Isotropy- generally, the biological mediums are anisotropic due to both the cellular structure and to the manner of cell connections; usually, the anisotropy of the tissues with long cells, such as ribbed muscle tissue or neuronal axons, is taken into account.

Homogeneity- the biological mediums are inhomogeneous, but generally it is assumed that the tissue is homogeneous on its sub-domains.

Linearity of the response to the usual stresses of the organism in magnetic and electric fields; the magnetic permeability μ, the electric conductivity σ and the electric permittivity ε are constant parameters.

Dependence on conditions- the values of ε, σ and μ depend on a series of medium characteristics, such as temperature, water content, chemical composition, the electromagnetic field characteristics and the integrity of the studied tissue.

2.5.1. Electric properties of human tissue

The electric properties, the electric conductivity σ and the electric permittivity ε (or the resistivity $\rho = 1/\sigma$), defined for unit volume of matter, characterize the behavior of a material or a medium brought inside the electric field.

The human body can be considered as a linear conducting volume of resistive nature and homogeneous on segments. Most of the tissues are isotropic. The muscle tissues and the brain tissues are considered anisotropic.

2.6. Magnetic phenomena at heart level

The electric currents are always associated with the magnetic fields produced by them. In 1819, Oerstad discovered the connection between electricity and magnetism, and in 1820 Biot and Savart state: the electric current induces a magnetic field that surrounds the current conductor, a law also valid for biocurrents. Therefore the biocurrents also generate biomagnetic fields.

2.6.1. Nature of biomagnetic sources

The source for magnetocardiogram (MCG) or Magnetoencephalogram (MEG) is determined by the electric activity of the heart muscle or of nervous cells.

2.6.2. Current sources

A current variable in time and space generates a magnetic field whose direction is given by the right hand rule.

2.6.3. Infinite and homogeneous conducting volume

2.6.4. Finite and inhomogeneous conducting volume

2.6.5. Relation between ECG and MCG

2.6.6. Relation between ECG and MCG

The main difference between the physical principles laying at the basis of ECG and MCG measurements is given by the fact that MCG is generated by the sum of all the currents inside the living organism, while ECG is only generated by the presence of the extra-cellular currents.

2.6.7. Importance of ECG and MCG diagnosis

ECG is the technique mostly used in cardiac diagnosis. It is a non-invasive technique, but implies a direct contact with the patient skin by means of electrodes (a disadvantage for the patients with burns, prematurely born children or for persons allergic to the contact with other objects).

At present, MCG is rather in an investigation stage, it was not implemented in clinical studies even if there are centers where this technique is currently executed. The main advantages of this technique are non-invasivity and contactless detection of useful information.

2.7. Conclusions

The theoretical researches concerning the bio-genesis of the biomagnetic field are being approximated with a quite reduced precision. Realization of models that imitate the bioelectric activity are closer to reality than the models destined to imitate the biomagnetic activity.

The physical models of the heart are even farther of reality. The magnetic field can be simulated by placing magnetic dipoles of different moments inside a volume surrounded by an imaginary thorax (Chapter 3).

Chapter 3.
Personal researches on the realization of models for biomagnetic field sources

3.1. Studies concerning the magnetic field distribution inside a conducting volume

The magnetic field distribution inside a conducting volume can be experimentally revealed by means of a model of the conducting volume. In this case the conducting volume was considered to be an approximation of the shape of His fascicle- a specialized conducting structure at the heart level.

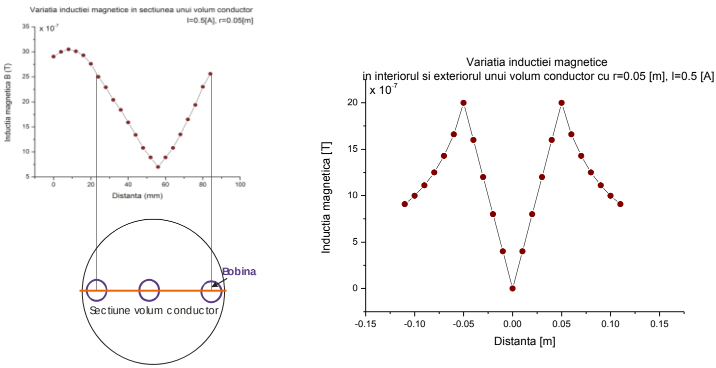

Figure 3.6. Magnetic field inside the conducting volume (left- measured values, right- calculated values)

One can notice that the measured values present small differences as compared to the analytically computed values; these differences appear due to the inherent errors of the used equipment or to small disturbances existing at the moment of measurements.

3.2. Studies concerning calculus of magnetic induction created by conducting cells

The electric conductor from the human body, the simplest and mostly used in modeling is the neurons axon, by whose means the nervous influxes are transmitted from the level of brain cortex to the organism and vice versa.

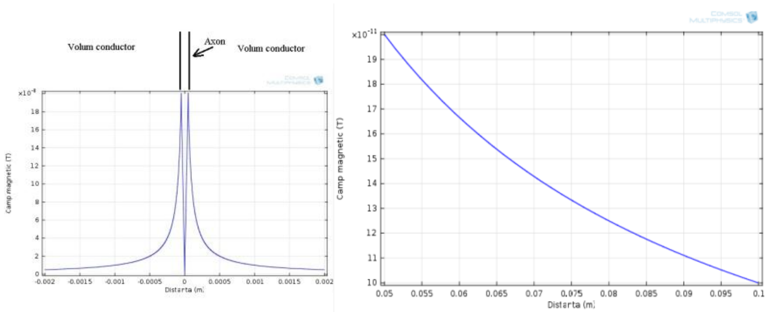

Fig. 3.8. Variation of the magnetic induction created by axon stimulation vs. distance

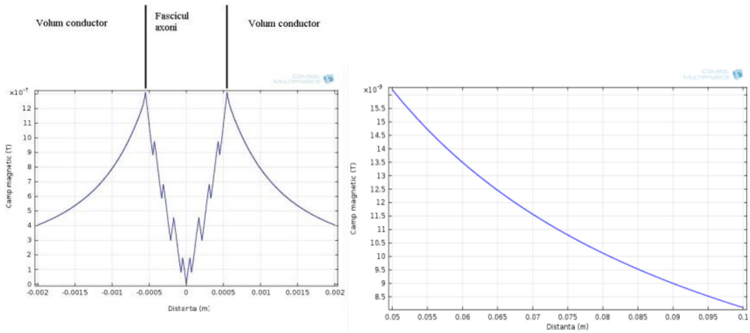

Fig. 3.11. Magnetic induction created by an axon fascicle- cross section

From these studies on the virtual model, one can notice that a single excitable cell produces at the distance x= 5 cm from its center a magnetic field equal to $20 \cdot 10^{-11}$ T, while a fascicle of excitable cells through which the depolarization front passes at the same time, produces at the distance x= 5 cm a magnetic field two order of magnitude higher, i.e. $16 \cdot 10^{-9}$ T, much easier to be detected by the SQUID sensor.

3.3. Studies concerning the modeling of heart electric and magnetic activity

The model of the heart as an organ refers to a tri-dimensional heart-thorax model that contains real heart and thorax geometries. The heart presents a complex geometry, its reproduction by means of the CAD type programs being difficult, such that simplified models are used, depending on the parameters investigated in the model.

The cardiac cycle is approximated through a series of curves corresponding to the P waves, complex QRS and T wave. In order to obtain results as close to reality as possible, we considered as reference and starting point of the magnetic field analysis and modeling, the representation given by the ECG SIM software, an interactive simulation software that permits to study the relation between the myocardium activity and the potentials appeared at the thorax surface [156].

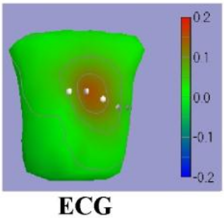	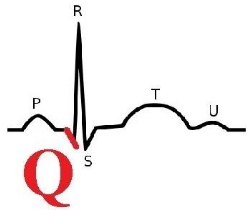
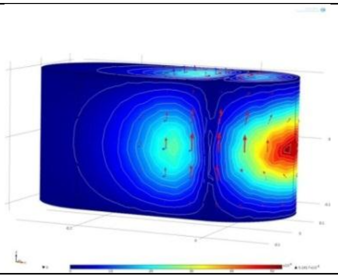	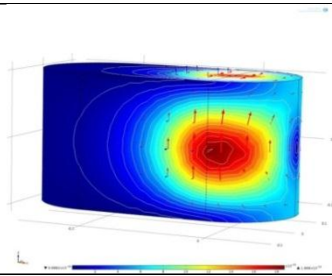
Q Wave – electric field Comsol	Q Wave – magnetic field Comsol

Fig. 3.19. Magnetic and electric field representation at the thorax surface- Q wave

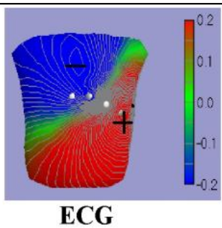	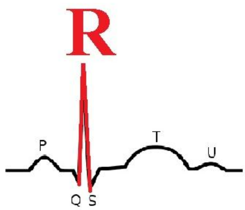

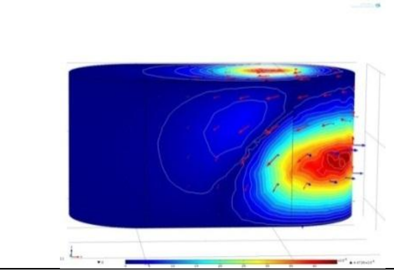	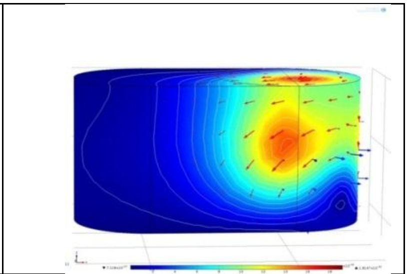
R Wave – electric field Comsol	R Wave – magnetic field Comsol

Fig. 3.20. Magnetic and electric field representation at the thorax surface- R wave.

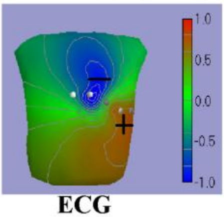	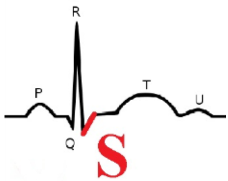
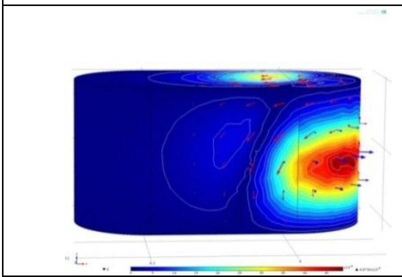	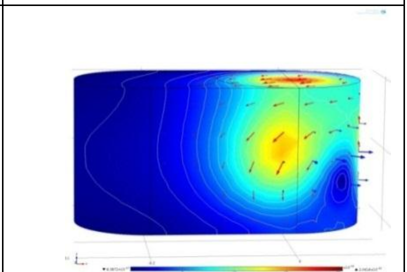
S Wave – electric field Comsol	S Wave – magentic field Comsol

Fig. 3.21. Magnetic and electric field representation at the thorax surface- S wave.

3.4. Simulation of an ECG signal

A code of ECG signal generation was realized by means of the Matlab software

3.5. Conclusions

Taking into account the proposed objectives, we have performed an experimental study on the magnetic field variation inside a conducting volume.

The magnetic field variation in cross section and at a distance was also studied for a virtual model produced by means of Comsol Multiphysics software for an axon-specialized conducting cell and for an axon fascicle.

The magnetic field variation at the surface of a virtual thorax model was also studied. The source of the biomagnetic field was considered to consist of an electric dipole located in the heart center, whose dipole moment rotates in space reproducing the motion of the heart vector during the cardiac cycle. Following the heart magnetic activity modeling, the values of the magnetic field were obtained at the thorax surface, almost equal to those obtained as the result of biomagnetic field measurements. This model can also be used in didactic purposes for the understanding of magnetic map modification at the thorax surface.

Chapter 4.
Researches concerning the influence of disturbances on biomagnetometric measurements

4.1. Influence of magnetic disturbances created by different conducting structures on a SQUID gradientmeter

The goal of this study is to determine the conditions in which a SQUID biogradientmeter can be used for biomagnetic measurements in an unshielded space and to what extent the circuit for electric power supply of the medical equipment disturbs the SQUID operation, as well as how can be ensured the biomagnetometer compatibility with the medium.

In this study various disturbance sources existing in the laboratory: parallel electric conductors, twisted conductors and a circular coil were analyzed, searching for the optimum version that permits to diminish the distortions level in biogradientmeter detection area.

If the disturbance source consists of only one conducting wire, the magnetic induction B and the magnetic field gradient G have the same value at any measuring point located on the circle circumference. This case can be found in the situation when the supply conductor enters the laboratory through a certain place, and comes out through another place, a case hardly met in practice, but taken into account in the performed study.

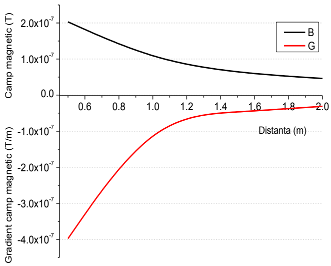

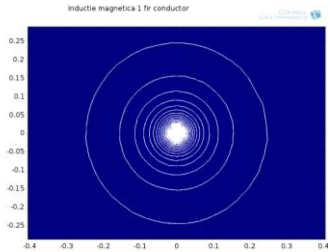

Figure 4.2. Magnetic field B and magnetic field gradient G- one conductor

Figure 4.3. Magnetic induction created by a conductor placed in the system center (Comsol model)

A second case is considered, when the disturbance source is represented by two parallel conductors located at a certain distance from one another. The two parallel conductors are considered located in the XY plane at a distance *d* from each other. The magnetic field and magnetic field variation are investigated in different measuring points located at the distance R from the center of the system in which the two conductors are located [112].

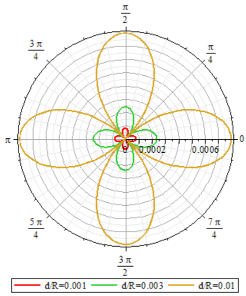

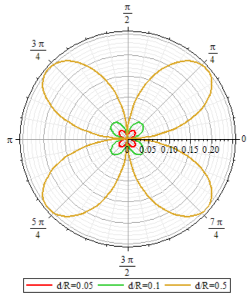

Fig. 4.7. Graphical representation of the component By for various values of the d/R ratio

Fig. 4.8. Graphical representation of the component By for various values of the d/R ratio

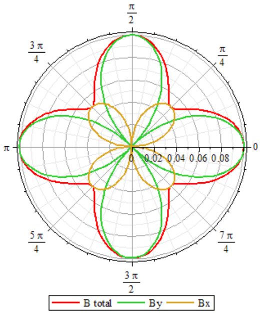

Fig. 4.9. Graphical representation of total B and the components Bx and By

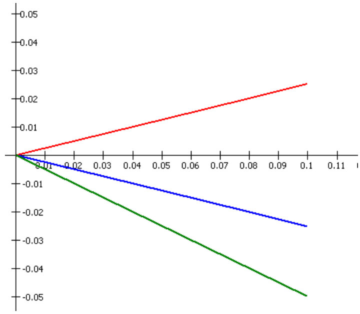

Fig. 4.10. Magnetic field gradient created by two conducting wires reported to the gradient created by a single conductor

In Fig. 4.10 we represented with green line Gx for $\theta = 45^o$; blue line- Gy for $\theta = 0^o$ and red line – Gy for $\theta = 90^o$.

The results obtained from the calculation led to the conclusion that two conducting wires generate at a certain distance from them a magnetic field that varies in terms of the ratio d/R. The smaller the ratio between the distance between the two conductors and the measurement distance, the smaller the magnetic field value. As the results of the analytical calculations and the graphical representations, one can draw the conclusion that By component has bigger values as compared to Bx component of the magnetic field. The total magnetic field presents minimum values for directions corresponding to the angles π/4, 3π/4, 5π/4 and 7π/4.

Another disposition of the two conductors was also considered, in a twisted arrangement, but this solution is not satisfactory due to the high value of the dispersion field, such that we studied the variant in which the two conductors are located in close parallel planes, but in a "meandering" form [98].

The radial and axial field components generated at the distances x= 2m and x= 1m were also calculated for the case when the conductors are disposed in parallel planes in the immediate proximity, in a "meander" form, with loop diameter d= 0.0045 m and I= 0.5 A.

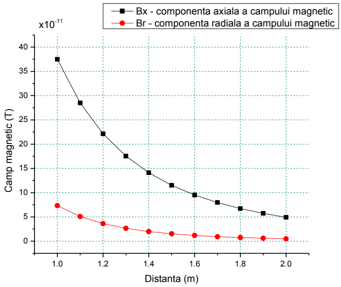

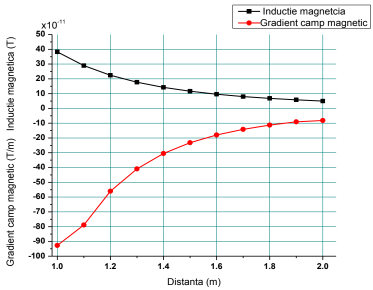

Fig. 4.18. Magnetic field- Bx and By components - 2 "meander" conductors

Fig. 4.19. Magnetic field B and magnetic field gradient G - two "meander" conductors

4.2. Studies of the shielding factors in the frequency range for various types of shields

In this study the magnetic field variation for various screening geometries made of aluminum was investigated.

4.2.1. Determination of the shielding factor for a cylindrical screen

A study on model concerning magnetic field attenuation when passing through different shield geometries and thicknesses was carried out. Aluminum was chosen as material for shields construction. An aluminum cylindrical shield was modeled, with the radius R= 0.5m, length of L= 1m and wall thickness of 0.012 m, in order to investigate the variation of damping factor in terms of the frequency of the applied magnetic field. The virtual model was produced by means of the Comsol Multiphysics software.

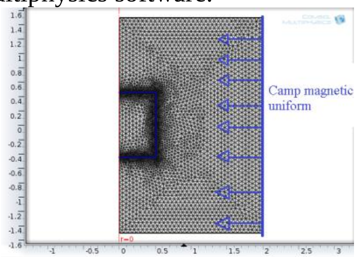

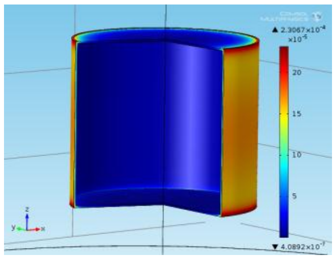

Fig. 4.32.The geometry of the model 2D

Fig. 4.33. The geometry of the model 3D

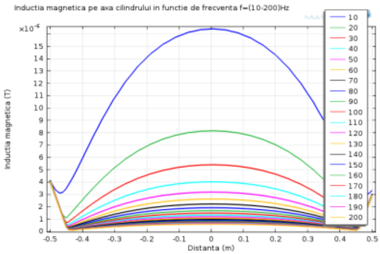

Fig. 4.34. Magnetic field variations along the central vertical axis in terms of frequency for a cylinder with closed ends

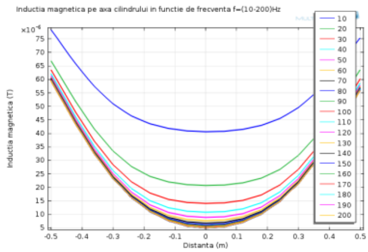

Fig. 4.35. Magnetic field variations along the central vertical axis in terms of frequency for a cylinder with open ends

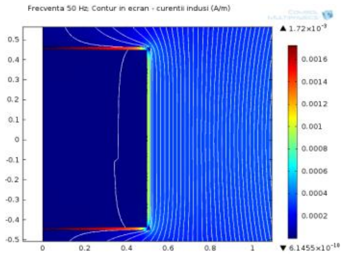

Fig. 4.39. Variation of the magnetic field attenuation when crossing a cylindrical shield closed at both ends; f= 50 Hz

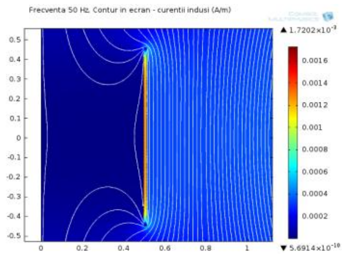

Fig. 4.38. Variation of the magnetic field attenuation when crossing a cylindrical shield open at its ends; f= 50 Hz

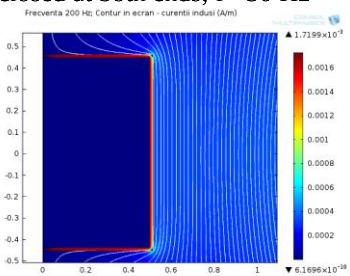

Fig. 4.41. Variation of the magnetic field attenuation when crossing a cylindrical shield closed at both ends; f= 200 Hz

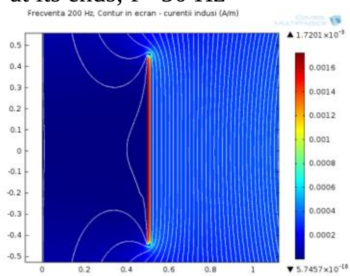

Fig. 4.40. Variation of the magnetic field attenuation when crossing a cylindrical shield open at its ends; f= 200 Hz.

4.2.2. Determination of the shielding factor for a spherical screen

The shield thickness was established at 0.012 m, and the inner radius of the sphere was 0.5 m. The shield thickness can be modified in order to study the variation of the damping factor in terms of shield thickness. The shield size and the type of field source were chosen considering also the computing power of the computer on which the simulation was performed, such that to avoid errors when processing the data and graphics.

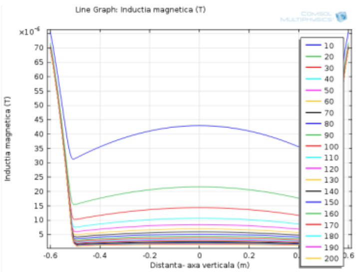

Fig. 4.45. Magnetic field variation vs. frequency in the center of the spherical shield-vertical axis; shield thickness 12 mm

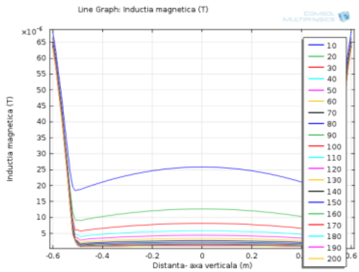

Fig. 4.46. Magnetic field variation vs. frequency in the center of the spherical shield-vertical axis; shield thickness 20 mm

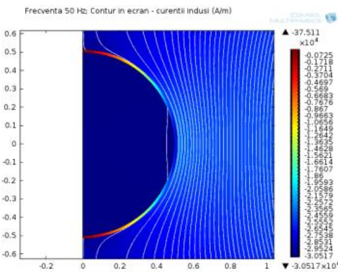

Fig. 4.49. Variation of magnetic field attenuation when crossing the shield; white lines- magnetic field lines; f= 50 Hz

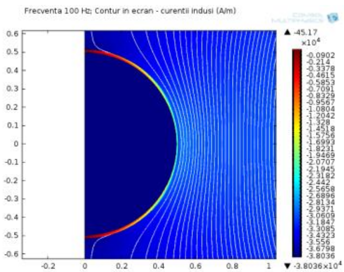

Fig. 4.50. Variation of magnetic field attenuation when crossing the shield; white lines- magnetic field lines; f=100 Hz

One can notice the appearance of the eddy currents induced within the shield and the absence of the magnetic field lines inside the space protected by the shield. The main goal of this study was to highlight the appearance of the eddy currents within the shield wall thickness and the diminution of magnetic field amplitude when crossing an aluminum shield. Aluminum was chosen as shield material since the shielded room from the Laboratory of Bioelectromagnetism BIM was manufactured of the same material.

4.3. Conclusions

The level of disturbances produced by the electric conductors depends on the conductor geometry and position with respect to the measuring system. Two geometries were studied for the structure with two conductors used for direct current and single-phase alternative current supply of the laboratory installation. The most adequate geometry from the standpoint of the disturbance level is that of the conductors disposed in a “meander” type arrangement. In practice, a twisted conductor geometry is used, since it is easier to accomplish.

Chapter 5

Installation destined to biomagnetometry studies. Laboratory of bioelectromagnetism. Description. Performances

5.1. Description of the installation destined to bio-electromagnetism studies. Laboratory of bioelectromagnetism- BIM

At the Faculty of Medical Bioengineering (BIM) of the University of Medicine and Pharmacy of Iassy there is the only laboratory of bio-electromagnetism that is equipped with a complex installation destined to biomagnetic field detection, a completely functional installation.

5.1.1. Study of biomagnetometry installation emplacement

Knowing the magnetic field variation inside the laboratory is very important to become aware of the sources of external disturbances existing in the immediate proximity of the SQUID magnetometer, the values of these disturbances and the moment of the day when they occur, such as to ensure an optimum organization of the monitoring activity.

5.2. Magnetic field distribution inside the shielded room

A study concerning the magnetic field distribution inside the shielded room was carried out; the magnetic field components along the three directions were measured by means of a triaxial magnetometer. The measurements were performed in the horizontal plane at 1 m distance from the floor of the shielded room, covering a surface of (250 x 250) cm^2 in a network of (5 x5) cm.

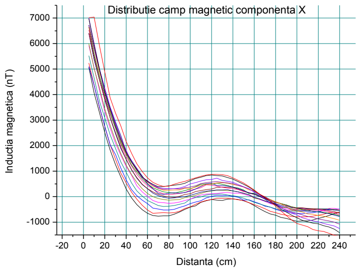

Fig. 5.10. Magnetic field distribution- X component

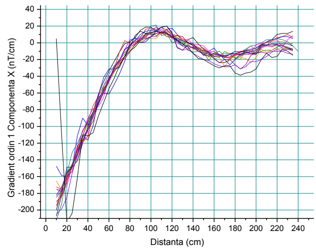

Fig. 5.13. Variation of the 1st order gradient- X component

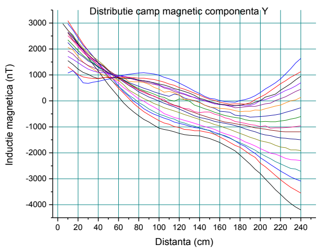

Fig. 5.11. Magnetic field distribution- Y component

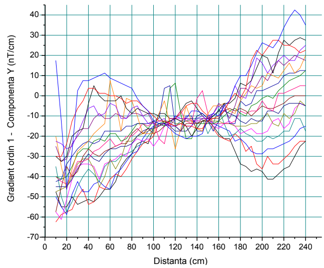

Fig. 5.14. Variation of the 1st order gradient- Y component

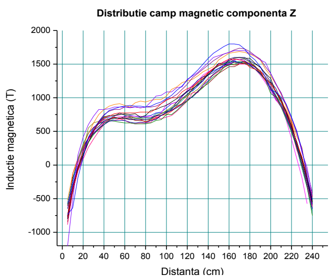

Fig. 5.12. Magnetic field distribution- Z component

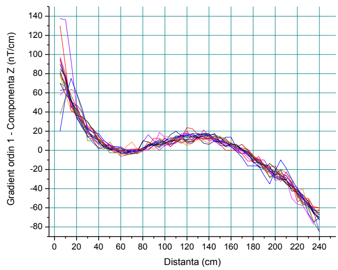

Fig. 5.15. Variation of the 1st order gradient- Z component

In the plane that passes through the center of the imaginary volume, in the zone of interest, the gradients corresponding to the three directions have the following values: Gx values vary between 20 nT/cm and -20 nT/cm; the values of the component Gy are smaller than 20 nT/cm, and Gz varies between 5 and -25 nT/cm. The magnetic field along the three directions can be considered as consisting of a continuous component and a variable component; as the continuous component is compensated by means of the magnetic field compensation system, only the time changing values of the magnetic field and the existing magnetic field gradients inside the investigated volume are of interest.

5.2.1. Shielded room

The shielded room has the dimensions of (3x2x2) m and it is built of aluminum sheets, the size of a sheet being (1x2x0.012) m. The aluminum sheets are joint together with bronze and brass screws. The room is fixed on a wood scaffolding such that to be positioned at the mid distance between the floor and the ceiling.

The air ventilation inside the shielded room is performed through two air hole shielded with a dense metallic wire mesh with small eyes; the air holes are situated on opposite walls at different heights, such that the air penetration within the shielded room is realized through the upper air hole, and its elimination through the lower air hole, in order to avoid the dust penetration. The air penetration hole is endowed with a filter for particles to avoid the air contamination inside the shielded room. The illumination of the shielded room is provided by means of d.c. supplied white LED sources (as they have a low consumption, the generation of electromagnetic disturbances in the proximity of the SQUID sensor will be avoided) [113].

5.2.2. Determination of damping factor for an aluminum shield

A theoretical study was carried out by means of the Maple software to investigate the modification of the damping factor for various types of shielding of different thicknesses. The shielded room from the Bioelectromagnetism Laboratory is made of 12 mm thick aluminum sheets, this being also the reason for studying this type of material.

The measurements have showed that at the frequency of 50 Hz the damping factor is ~20 dB. From the above calculations and the graphics presented in Figure 5.22, it follows that at the same frequency the damping factor is equal to 8.6 dB. The difference of 11.4 dB corresponds to an additional damping introduced by the magnetic fields generated by the eddy currents induced in the walls of the shielded room.

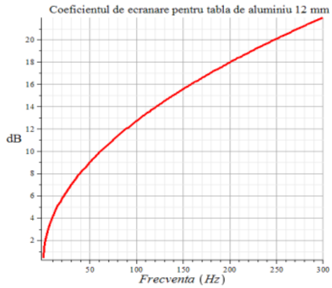

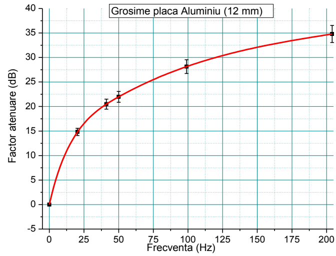

Fig. 5.22. Variation of the damping factor with frequency for a 12 mm thick aluminum shield

Fig. 5.23. Damping factor of the 12 mm thick Al sheet [121]

5.2.3. Study on modification of magnetic field phase when crossing an aluminum shield

The phase variation inside the shielded room presents a great importance for the right operation of the compensation system that works in a negative feed-back loop, whose magnetic field sensors are situated inside the shielded room; the modification of the magnetic field phase must be correlated with the phase of the field created by the system for magnetic field active compensation. This phase modification depends on the position of the magnetic field sensor inside the room, position that needs to remain steady all along the biomagnetic measurements [124].

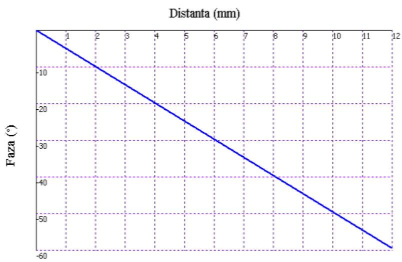

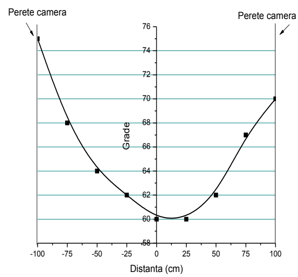

Fig. 5.25. Phase within the 12 mm thick Al shield- frequency 50 Hz.

Fig. 5.26. Magnetic field phase inside the shielded room- Oy direction [124]

The presence of the Foucault currents induced within the wall determines the appearance of a magnetic field component that sums up with the magnetic field at the exit from the wall. The field determined by the Foucault currents is also out of phase as compared to the incident field. In consequence, the phase of the residual field beyond the shield wall presents an apparent anomaly.

Knowing the residual field phase is important for the operation of system for field control and compensation through negative feedback.

5.3. System for ambiental magnetic field control

The ambiental magnetic field can be compensated by means of a triaxial system of large size Helmholtz coils, inside which a volume with diminished and constant magnetic field value is created. The Helmholtz coil system can be configured with a circular or square shape. Given the reduced available space and the necessity of the largest volume possible with uniform magnetic field, we opted for a square configuration of the Helmholtz coil system, to be able to use as much space as possible both in the vertical and horizontal direction.

The compensation of the local magnetic (geomagnetic) field components is accomplished by using two independent systems: a manual and an automated system.

The compensation range of the automated system is of ±5 μT, the maximum current being ± 1 A [119, 120]. The manual compensation permits to diminish the ambiental field down to 1- 2 nT.

5.4. SQUID Biogradientmeter

The utilized SQUID gradientmeter is of the type HITS SQUID Magnetometer model 703 produced by Tristan Tech., with the magnetic sensors connected such that to obtain three channels for the 1st order gradient and one channel for the 2nd order gradient, with electronic subtraction. The SQUID gradientmeter is fastened on the ceiling of the shielded room by means of a system that allows its positioning at different heights, being also able to move on a horizontal plane. It is advisable that the SQUID device remains in a fixed position all along the measurements, to avoid introducing an additional noise due to magnetic field sensors. In order to produce the magnetic maps of the field at the surface of the subject, the bed with the patient can move in the horizontal plane.

5.5. Conclusions

Following the proposed objectives, it was established that the location is generally adequate, i.e. there is indeed a disturbing magnetic field, but it can be diminished using the chosen solutions. It was found out that the residual magnetic field inside the shielded room with the frequency of 50 Hz is reduced due to two effects: by means of the absorption within the room walls, and by compensation through the fields generated by the eddy currents.

The field generated by the Foucault currents and the residual field emerging from the room walls have the phase changed as compared to the outside field. Therefore, within the room volume a residual field is found whose phase is variable.

The measured gradient differs from the gradient computed for a dipolar source, due to the volume bounded by the two sensing coils.

The electromagnetic compatibility of the installation for MCG is provided through two methods and means:

- The first consists in the utilization of a shielded room made of a non-ferromagnetic material, namely aluminum, with wall thickness big enough to reduce the alternative fields starting from the industrial frequencies (50 Hz). The ambiental continuous or slowly variable magnetic fields are reduced by means of the magnetometric installation of magnetic field compensation and control.
- The second method is a static shielding method that makes use of the shielding properties of conductible materials with large enough thickness. The shielding range stretches from the audio-frequencies to frequencies of the order of GHz.

Chapter 6.
Experimental researches of magnetocardiography. Processing of magneto-cardiographic signals

6.1. Recording a magnetocardiogram- MCG

Once knowing the level of magnetic disturbances and their variation during a 24 hours period, in order to improve the signal to noise ratio, it is recommended to perform the magnetocardiographic recording during the time interval when the magnetic disturbances are minimum (starting with 17^{oo} till 6^{oo} next day).

Fig. 6.1.Recording setup for a magnetocardiogram. View from the shielded room

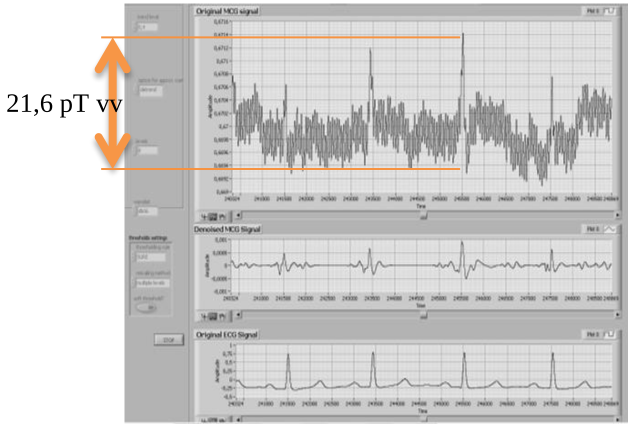

Fig. 6.2. Unfiltered MCG signal, filtered MCG and ECG- reference signal [121]

6.2. Magnetocardiogram processing

The stages of magnetocardiogram recording are as follows:

- diminish the level of ambiental magnetic field and of magnetic disturbances;
- signal detection;
- record the primary signals
- signal processing;
- signal interpretation by specialized medical personnel.

The signal processing implies transformation techniques applied to the signal, meant to eliminate the noises from the mains, artifacts, as well as the detection of certain frequencies, application of filters, all these in order to obtain a signal without artifacts, yet preserving the information necessary to an accurate diagnosis.

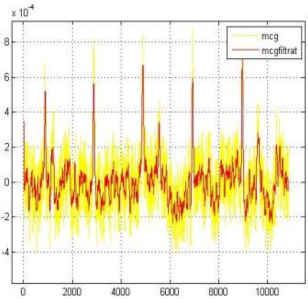

Fig. 6.7. Filtered MCG signal (red line), unfiltered MCG (yellow line)

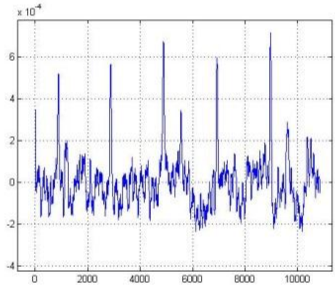

Fig. 6.8. MCG signal filtered with Savitzky- Golay filter

6.3. Processing the MCG signal by means of Wavelet transform

The Daubechies Wavelet functions are adequate for the analysis of the biosignals characterized by a sharp peak, because they have less stored energy in high frequency band. Most of the information useful for the ECG- MCG diagnosis is found within the intervals and amplitudes of the P-QRS-T waves.

By accessing from the control interface of the Matlab program, the filtered MCG signal is loaded, with its previously corrected basis, in order to determine the coefficients of the Daubechies function.

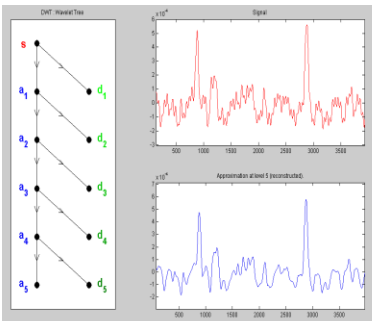

Fig. 6.4. The way in which the Wavelet transform db 6 Level 5 approximates the MCG signal

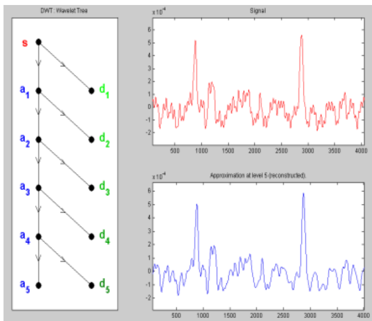

Fig. 6.5. The way in which the Wavelet transform db 5 Level 5 approximates the MCG signal

Taking into account the signal processing techniques presented in Chapter 1, from the five introduced methods we only realized MCG signal processing using the Wavelet transform, because the signal was acquired by means of a single channel system. The PCA (Principal Component Analysis) and ICA (Independent Component Analysis) methods can only be applied in the case when there are at least two sources of MCG signal, which implies the existence of a multichannel SQUID device.

6.4. Methods of magnetic mapping - fetal magnetocardiography

The magnetic mapping method can also be applied in the case of detecting the magnetic signal produced by the fetal heart (fMCG). A grid was proposed with (3x3) measuring point, with the center in the umbilical zone (Fig. 6.20).

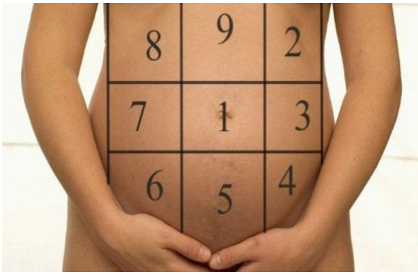

Fig. 6.20. Grid proposed for fetal magnetocardiography detection [123]

6.5. Conclusions

The objectives of the study presented in this chapter were:

- establish a protocol for the acquisition, processing and filtering of the acquired MCG signal
- establish a technique for fMCG signal detection under the condition that the exact fetus position within mother womb is not known.

Taking into account the proposed objectives, I presented a protocol that needs to be complied with, in order to acquire a MCG signal in the conditions offered by the Laboratory of Bioelectromagnetism, as well as the techniques for processing and filtering the acquired MCG signal. I also presented a grid proposed for the detection of the fMCG signal on the conditions that its detection with an echoDoppler device was impossible.

7. General conclusions

Considering the objectives proposed in drawing up this Thesis, I have accomplished the following:

1. A documentary study on the types of high resolution magnetometers that can be used in biomedical area. A documentary study concerning the state of art in the world of the methods and means to detect, record and analyze the biomagnetic sounds, as well as the performances reached by the biomagnetic installations operating worldwide.

2. A theoretical and experimental study was performed on the physical principles involved in the genesis of bioelectric and biomagnetic field, by whose means the values of the electric and magnetic fields can be represented in different stages of the cardiac cycle. The parameters used to define the model can be modified any time, or one can carry out post-processing studies by modifying some parameters, in order to highlight the modifications that appear in certain pathological situations.

3. The magnetic field variation was studied at the surface of a virtual thorax model produced by means of the Comsol Multiphysics software. The biomagnetic field source was considered to be represented by a dipole located in the heart center, whose dipolar moment rotates in space, reproducing the motion of the cardiac vector during the cardiac cycle. Following the modeling of the cardiac magnetic activity, the values of the magnetic field at the thorax surface were obtained and they were approximately equal to those obtained during the biomagnetic measurements. This model can also be used in didactic purposed in order to understand the modifications of the magnetic map at thorax surface.

4. A study of the electromagnetic compatibility and of the emplacement of the mains conductors was also carried out, concerning the disturbances they produce to the laboratory electromagnetic medium.

5. The variation of the damping factor for various shield shapes and configurations was also studied.

6. A study on the Bioelectromagnetism Laboratory emplacement was also performed, measuring the magnetic field in different locations, in order to choose the optimum space destined for biomagnetometry studies. The theoretical study and experimental results concerning the level of the electromagnetic field outside and inside the shielded room indicated satisfactory levels for the residual magnetic and electromagnetic fields.

7. The conditions in which a gradientmeter is able to detect a signal generated by the human cardiac activity in the presence of the disturbing magnetic fields were determined.

8. A protocol was established for processing a biomagnetometric signal generated by the cardiac electric activity.

BIBLIOGRAPHY

[1] Andra W. and Nowak H., Magnetism in medicine, WILEY – VCH Verlag GmbH&Co. KGaA, Weinheim 2008

[2] Malmivuo Malmivuo J., Plonsey R., Bioelectromagnetism: Principles and Appliactions of Bioelectric and Biomagnetic Fields, Oxford University Press, New York, 1995

[3] Curs 1 Compatibilitate electromagnetică – prof dr Dan Pitica-Universitatea Cluj

[4] John S. Scott, Introduction to EMC, ISBN 0 750631015, Newnes 2005

[5] Kajiwara G., Harakawa K., Ogata H., ”High performance magnetically shielded room„, IEEE Trans.on Mag., vol.32, pp.2582-2585, 1996

[6] Kato K., Yamazaki K., Matsuba H., Sumi C., Sato S., ”Active magnetic shield for biomagnetic measurement”, Proc. of the 12th Int. Conf. on Biomagnetism, 2000, Nenonen J, Ilmoniemi R, Katila T, editors. 2000 Aug 13-17, Espoo, Finland. Helsinki Univ. of Technology; p. 965-967

[7] C. Holmlund, M. Keipi, T. Meinander, A. Penttinen, H. Seppa, „Novel concepts in magnetic shielding”, Proc. Of the 12th Int. Conf. Of Biomagnetsm 2000, Nenonen J, Ilmoniemi R, Katila T, editors. 2000 Aug 13-17, Espoo, Finland. Helsinki Univ. of Technology; pp. 968-969.

[8] Alldred J.C.. Scollar I., „Square cross section coils for the production of uniform magnetic fields”, J.Sci. Instrum., vol.44, pp.755-760, 1967

[9] Cohen D., United States Patent 3,557,777 din 1971 – Magnetic study of bioelectric phenomena

[10] Resmer F., Nowak H., Giesler F., Haueisen J., „Development of an active magnetic screen to allow a biomagnetometer to be used in an unshielded environment”, Supercond. Sci. Technol., vol.17, 2004, pp. 1365-1371.

ISI papers

1. Banarescu Anca, Baltag Octavian, The Bragg diffraction modeling using ultrasounds, Conference: National Conference on Applied Physics Location: Galati, ROMANIA Date: JUN 09-10, 2006 Source: ROMANIAN JOURNAL OF PHYSICS Volume: 53 Issue: 1-2 Pages: 191-195 Published: 2008. Factor impact: 0.526, Factor influenta: 0.0931

2. Costandache D.; Banarescu A.; Baltag O., Rau I., Rau M., S. Ojica, Dynamic Shielding in Biomagnetism, Source: INTERNATIONAL CONFERENCE ON ADVANCEMENTS OF MEDICINE AND HEALTH CARE THROUGH TECHNOLOGY Book Series: IFMBE Proceedings Volume: 26 Pages: 121-124 DOI: 10.1007/978-3-642-04292-8_27 Published: 2009

3. Baltag O., Banarescu A.; Costandache D. M. Rau and S. Ojica, Microwaves and Infrared Thermography - Applications in Early Breast Cancer Detection, Source: INTERNATIONAL CONFERENCE ON ADVANCEMENTS OF MEDICINE AND HEALTH CARE THROUGH TECHNOLOGY Book Series: IFMBE Proceedings Volume: 26 Pages: 195-198 DOI: 10.1007/978-3-642-04292-8_43 Published: 2009

4. Baltag Octavian; Costandache Doina; Rau Miuta; Iftemie Anca, et al., Dynamic shielding of the magnetic fields, ADVANCES IN ELECTRICAL AND COMPUTER ENGINEERING Volume: 10 Issue: 4 Pages: 135-142 DOI: 10.4316/AECE.2010.04022 Published: 2010. Factor impact 0.552, Factor influenta 0.082

5. Rau Miuta, Iftemie Anca, Baltag Octavian,et.al., The Study of the Electromagnetic Shielding Properties of a Textile Material with Amorphous Microwire, Source: ADVANCES IN ELECTRICAL AND COMPUTER ENGINEERING Volume: 11 Issue: 1 Pages: 17-22 DOI: 10.4316/AECE.2011.01003 Published: 2011. Factor impact 0.552, Factor influenta 0.082

6. Ojica, S.; Iftemie. A, Rau, M. C.; et al., Microwaves and Infrared Thermography - Comparative Studies in Early Breast Cancer Detection, Conference: 7th International Symposium on Advanced Topics in Electrical Engineering (ATEE) Location: Bucharest, ROMANIA Date: MAY 12-14, 2011, Sponsor(s): Inst Elect & Elect Engineers (IEEE) Source: 2011 7TH INTERNATIONAL SYMPOSIUM ON ADVANCED TOPICS IN ELECTRICAL ENGINEERING (ATEE) Book Series: International Symposium on Advanced Topics in Electrical Engineering Published: 2011

Papers in the IEEE international base

1. Ojica, S.; Iftemie, A.; Rau, M.C.; Costandache, D.; Baltag, O., Microwaves and infrared thermography — Comparative studies in early breast cancer detection, Advanced Topics in Electrical Engineering (ATEE), 2011 7th International Symposium on Publication Year: 2011 , Page(s): 1 – 4.

2. Ojica, S.; Iftemie, A., Thermographic studies in vivo and in vitro for detection of tumor structures using microwave radiometry, Advanced Topics in Electrical Engineering (ATEE), 2013 8th International Symposium on Digital Object Identifier: 10.1109/ATEE.2013.6563430. Publication Year: 2013 , Page(s): 1 – 4. Acceptata spre publicare in International Journal of Monitoring and Surveillance Technologies Research (IJMSTR)

3. Iftemie, A. ; Ojica, S., Study on the magnetic perturbations caused by different configurations of the electrical conductors with applications in biomagnetometry, Advanced Topics in Electrical Engineering (ATEE), 2013 8th International Symposium on Digital Object Identifier: 10.1109/ATEE.2013.6563454. Publication Year: 2013, Page(s): 1 – 4

4. Ojica, Silvana ; Iftemie, Anca, Noninvasive assessment of breast pathologies during pregnancy, E-Health and Bioengineering Conference (EHB), 2013 Digital Object Identifier: 10.1109/EHB.2013.6707252 . Publication Year: 2013 , Page(s): 1 - 4